Performance Bounds for Maximum Likelihood Detection of Single Carrier FDMA [1]

Mark Geles, Amir Averbuch, Ofer Amrani and Doron Ezri

Abstract

Single carrier FDMA (SC-FDMA) plays an important role in modern wireless communications as an alternative to OFDM since mainly it exhibits low peak-to-average power ratio (PAPR). Hence, SC-FDMA is employed as the uplink scheme for the 3GPP long term evolution (LTE). In the presence of multipath, the SC-FDMA signal may arrive at the receiver perturbed by inter-symbol-interference (ISI). It is similar to other SC transmission schemes. This makes the standard single tap frequency domain equalization suboptimal. Optimal maximum likelihood (ML) detection for SC-FDMA is in most cases prohibitively complex, making it useful mostly as a performance bound for suboptimal detection schemes. In this work, the performance of the optimal decoder for SC-FDMA is analyzed. The analysis can be applied to a generalized SC-FDE scheme as well, however, in this paper we chose the SC-FDMA setting as a study case. Bit error rate (BER) closed form bounds are provided for low and high SNR regimes in correlated and uncorrelated Rayleigh fading channels. These bounds reveal that the diversity order at high SNR is significantly smaller than in low SNR regime. Moreover, error rate flaring behavior is demonstrated under optimal detection of SC-FDMA. The analytical results are verified by simulations.

Index Terms

Maximum Likelihood, Single Carrier FDMA.

I. Introduction

SINGLE carrier FDMA (SC-FDMA) employs different orthogonal frequencies (sub-carriers) to transmit information symbols. However, the information symbols undergo discrete Fourier transform (DFT) prior to their allocation to sub-carriers. This approach produces a single carrier-like waveform which reduces considerably the envelope fluctuations of the time domain signal. Therefore, SC-FDMA signals exhibit inherently lower PAPR than what OFDM signals exhibit. The PAPR advantage does not come without cost: in the presence of multipath propagation, the SC-FDMA signal may arrive at the receiver with a significant ISI, even when the delay spread is smaller than the cyclic prefix.

M. Geles and O. Amrani are with the Department of Systems Electrical Engineering, Tel Aviv University, Tel Aviv 69978 Israel

A. Averbuch is with the School of Computer Science, Tel Aviv University, Tel Aviv 69978 Israel

D. Ezri is with Greenair Wireless, 47 Herut St., Ramat Gan, Israel

A practical SC-FDMA detector usually involves a single tap frequency domain equalizer (FDE) followed by the application of the inverse DFT (IDFT). Frequency domain minimum mean square error (MMSE) is most commonly employed while other linear detectors, such as zero forcing (ZF), are also possible. However, linear detectors are suboptimal in severe multi-path environment for distributed SC-FDMA and localized SC-FDMA.

Non-linear detection of SC-FDMA has attracted considerable attention [1]. More advanced SC-FDMA detection schemes, whose performance lie between those of MMSE and MLD, have been proposed. Turbo equalization (TEQ) [2] and frequency domain TEQ (FD-TEQ) [3] were proposed as natural candidates for SC-FDMA detection when channel coding is used [4], [5]. When TEQ is used, the equalizer and the channel decoder are implemented as soft input - soft output blocks, separated by proper bit interleavers. Information produced by one of these blocks is considered as a-priori information for the other, resulting with an iterative receiver structure. A different approach to SC-FDMA detection, which combines MMSE and MLD, has been recently proposed [6]. The receiver adopts the group interference suppression (GIS) technique in which groups of symbols, corresponding to highly correlated columns of $\boldsymbol{G}$ (see in Section II), are selected. Each group undergoes joint detection which follows a linear pre-filtering procedure aiming at suppressing the interference from all the other symbols.

Recent contributions analyzed the performance of several detection schemes applied to SC-FDMA transmission for various channel models. Performance analysis of ZF and MMSE linear detectors, are given in [7]. In addition to the exact ZF and MMSE bit error rate (BER) formulae, an upper bound on the packet error rate (PER), under maximum likelihood detection (MLD), is given in [8]. Therein, a packet means a series of modulated symbols allocated to the DFT block (per user). Since an erroneous packet may include any number of erroneous bits, derivation of BER performance from the PER is not trivial. In both papers, [7] and [8], the expressions are given as functions of the fading channel realization rather than the channel statistics, hence the average error rate is not provided.

For evaluating the effectiveness of the aforementioned detection schemes, it is useful to compare their performance with those of the optimal MLD. MLD performance evaluation via computer simulations has an exponential complexity. This motivates the need to derive its performance analytically. In this work[1], we present tight lower bounds on the bit error probability of the ML detection of SC-FDMA assuming Rayleigh-fading channel. The bounds are calculated by integrating of the selected error-vector probabilities w.r.t. the fading channel distribution function. The closed form expressions derived herein depend only on the size of the DFT. BER flaring is revealed by both analysis and simulations. It shows that the diversity order in high SNR regime is significantly lower than the diversity order in the low SNR regime.

[1]Preliminary results were reported in [9]

The rest of the paper is organized as follows. Section II contains a description of the SC-FDMA system. In Section III we develop closed-form bounds on the BER performance for ML detection of SC-FDMA. Section IV contains simulation results that provide additional support for the theoretical results obtained in Section III. Section V concludes the paper.

II. SC-FDMA System Description

By considering an SC-FDMA system with N sub-channels and a adequate cyclic prefix, the received signal in the nth sub-channel is

$$y_n = h_n\, x_n + \rho\, w_n, \tag{1}$$

where h_n represents the channel experienced by the nth sub-carrier, x_n is the nth element at the DFT output transmitted on the nth sub-carrier and $\rho\, w_n$ is an additive white Gaussian noise with zero mean and variance ρ^2. In a matrix form, the signals received (on all sub-carriers) can be written as

$$\boldsymbol{y} = \boldsymbol{H}\boldsymbol{x} + \rho\, \boldsymbol{w}, \tag{2}$$

where $\boldsymbol{y} = [y_1, \ldots, y_N]^T$, $\boldsymbol{H} = \text{diag}\left\{[h_1 \ldots, h_N]^T\right\}$, $\boldsymbol{w} = [w_1, \ldots, w_N]^T$ and $\boldsymbol{x} = [x_1, \ldots, x_N]^T$ is the DFT output vector

$$\boldsymbol{x} = \boldsymbol{F}\boldsymbol{s}, \tag{3}$$

where $\boldsymbol{F}$ is the unitary $N \times N$ DFT matrix and $\boldsymbol{s}$ is $N \times 1$ vector of symbols taken from a (normalized) constellation. By substituting (3) into (2), the received signal vector takes the form

$$\boldsymbol{y} = \underbrace{\boldsymbol{H}\boldsymbol{F}}_{\boldsymbol{G}}\boldsymbol{s} + \rho\, \boldsymbol{w}. \tag{4}$$

We first consider the simple case where the channel magnitude $|h_i| = |h|, i = 1, \ldots, N$, is constant within the occupied bandwidth. This corresponds, for example, to a localized transmission where the occupied bandwidth is significantly smaller than the coherence bandwidth of the channel or corresponds to a strong line of sight scenario. Here we have $\boldsymbol{H}^*\boldsymbol{H} = |h|^2\boldsymbol{I}$ and the composite matrix $\boldsymbol{G}$ satisfies

$$\boldsymbol{G}^*\boldsymbol{G} = (\boldsymbol{H}\boldsymbol{F})^*(\boldsymbol{H}\boldsymbol{F}) = |h|^2\boldsymbol{F}^*\boldsymbol{F} = |h|^2\boldsymbol{I}, \tag{5}$$

which means that the columns of $\boldsymbol{G}$ are orthogonal. For this case, linear equalization (e.g., ZF) is optimal [10].

We continue with the case where the channel magnitudes vary within the occupied bandwidth. This corresponds, for example, to a distributed SC-FDMA, or to a localized transmission occupying a bandwidth larger than (or of the order

of) the coherent bandwidth. Here, in contrast to OFDM, the columns of the composite matrix $\boldsymbol{G}$ are not orthogonal. Hence, linear detection is not optimal. The optimal solution is given by

$$\hat{\boldsymbol{s}}_{\text{ML}} = \underset{\boldsymbol{s}\in\mathscr{C}}{\operatorname{argmin}} \|\boldsymbol{y} - \boldsymbol{G}\boldsymbol{s}\|^2, \tag{6}$$

where $\mathscr{C}$ is the space of length-N vectors whose alphabet consists of the symbols drawn from the employed constellation. Although the MLD approach in Eq. (6) brings to the optimal solution, its calculation is impractical since its implementation complexity grows exponentially fast with N.

More practical, the MMSE receiver, which is typically suboptimal, computes the MMSE estimator

$$\begin{aligned} \tilde{\boldsymbol{s}}_{\text{MMSE}} &= \boldsymbol{G}^* \left(\boldsymbol{G}\boldsymbol{G}^* + \rho^2 \boldsymbol{I}\right)^{-1} \boldsymbol{y} \\ &= \boldsymbol{F}^* \boldsymbol{H}^* \left(\boldsymbol{H}\boldsymbol{H}^* + \rho^2 \boldsymbol{I}\right)^{-1} \boldsymbol{y}, \end{aligned} \tag{7}$$

where $(\cdot)^*$ denotes conjugate transposition and $\boldsymbol{I}$ is the identity matrix with the appropriate dimensions. The elements of $\tilde{\boldsymbol{s}}_{\text{MMSE}}$ are then *sliced*, i.e. hard detected, to obtain the estimates of the transmitted symbols. Using the fact that $\boldsymbol{H}$ is a diagonal matrix and $\boldsymbol{F}$ is the unitary DFT matrix, the MMSE estimator is simplified to become

$$\tilde{\boldsymbol{s}}_{\text{MMSE}} = \text{IDFT}\left\{[\hat{x}_1, \ldots, \hat{x}_N]^T\right\}, \tag{8}$$

where $\hat{x}_n$ is the MMSE estimator of the frequency domain

$$\hat{x}_n = \frac{h_n^*}{|h_n|^2 + \rho^2} y_n. \tag{9}$$

This means that the MMSE receiver can be considered as a single tap FDE followed by the application of the IDFT, which corresponds to an additional DFT operation at the transmitter.

III. Closed-Form Bounds on the ML Error Probability

In this section, we derive lower-bounds on the BER performance of maximum likelihood detection of SC-FDMA. We first derive the bounds for the uncorrelated fading channel for both low and high SNR regimes. Then, we bound the performance in a correlated channel.

A. Preliminaries

The deviation vector $\boldsymbol{e} \triangleq \tilde{\boldsymbol{s}}_{ML} - \boldsymbol{s}$ is defined as the difference between a source vector and the estimated vector. The probability associated with the deviation vector $\boldsymbol{e}$, given the channel matrix $\boldsymbol{H}$, is

$$\Pr\{\boldsymbol{e}|\boldsymbol{H}\} = Q\left(\frac{\|\boldsymbol{H}\boldsymbol{F}\boldsymbol{e}\|}{\sqrt{2}\rho}\right), \tag{10}$$

where

$$Q(x) = \frac{1}{\sqrt{2\pi}} \int_x^\infty \exp\left(-\frac{y^2}{2}\right) dy. \tag{11}$$

The performance of the classical OFDM setting under flat fading can be derived from Eq. (10) assuming that $\boldsymbol{F}$ and $\boldsymbol{H}$ are 1×1 matrices. In this case, $\boldsymbol{F} = 1$ and $\boldsymbol{H}$ is a scalar denoted by h. Assume WLOG that $h = 1$. Then, the error probability for the normalized QPSK satisfies

$$\Pr\{e|h\} = Q\left(\frac{\|1 \cdot 1 \cdot e\|}{\sqrt{2}\rho}\right) \leq Q\left(\sqrt{\text{SNR}}\right), \tag{12}$$

where $\text{SNR} \triangleq 1/\rho^2$.

Assume that n_e, $0 \leq n_e \leq N$ is the number of errors in the $N \times 1$ deviation vector $\boldsymbol{e}$. Then, the exact BER as a function of the channel realization $\boldsymbol{H}$ is

$$\text{P}_b(\boldsymbol{H}) = \frac{1}{N} E\{n_e|\boldsymbol{H}\} = \frac{1}{N} \sum_{n_e=1}^{N} n_e \cdot \Pr\{n_e|\boldsymbol{H}\}, \tag{13}$$

where $\Pr\{n_e|\boldsymbol{H}\} = \Pr\{\bigcup\{\boldsymbol{e} : \text{number of errors is } n_e\}|\boldsymbol{H}\}$ is the probability that the deviation vector $\boldsymbol{e}$ contains exactly n_e non-zero elements. In order to obtain an average over the statistics of a specific channel model, the expression (13) has to be averaged using the joint probability distribution function (PDF) of the channel vector $\boldsymbol{h} = [h_1, \ldots, h_N]^T$. Following this approach, the average BER is

$$\text{P}_b = \frac{1}{N} \sum_{n_e=1}^{N} n_e \cdot \int \Pr\{n_e|\boldsymbol{H}\} \Pr\{\boldsymbol{H}\} \, d\boldsymbol{H}. \tag{14}$$

By identifying the most dominant deviation vector $\boldsymbol{e}_o$, we can derive from Eq. (14) the following lower bound

$$\text{P}_b \geq \frac{1}{N} n_e(\boldsymbol{e}_o) \cdot \int \Pr\{\boldsymbol{e}_o|\boldsymbol{H}\} \Pr\{\boldsymbol{H}\} \, d\boldsymbol{H}, \tag{15}$$

where $\boldsymbol{e}_o = \underset{\boldsymbol{e} \in \mathscr{E}}{\text{argmax}}\{\int \Pr\{\boldsymbol{e}|\boldsymbol{H}\} \Pr\{\boldsymbol{H}\} \, d\boldsymbol{H}\}$ and $\mathscr{E}$ is the set of all possible deviation vectors. Note that even if the integral in Eq. (15) can be solved analytically, the bound itself is difficult to calculate due to the fact that there are $4^N - 1$ different deviation vectors. Therefore, this bound can be used in cases where the DFT size is sufficiently small.

There are cases for which we can explicitly calculate the bound defined in Eq. (15). In what follows, we derive closed form expressions for some of these cases. In the Rayleigh channel distribution case, the maximizer $\boldsymbol{e}_o$ in Eq. (15) can be found analytically.

In order to obtain the maximizer $\boldsymbol{e}_o$, we develop (in Sec. III-B) an upper bound on the probability of $\boldsymbol{e}$. Then, in Sec. III-C, we show that there exists a specific vector whose probability is greater than the upper bound on any other deviation vector. This vector is the maximizer $\boldsymbol{e}_o$.

B. Upper bound on the probability of a specific deviation vector in Rayleigh Channel

We adopt the classical correlated Rayleigh model [10], [11], which corresponds to a multipath environment. Specifically, we assume that $\boldsymbol{h}$ is a complex normal random vector with zero mean and covariance matrix $\boldsymbol{C}$ where $\det(\boldsymbol{C}) \neq 0$. Following this approach, the average probability for the deviation vector $\boldsymbol{e}$ is

$$\begin{aligned} \Pr\{\boldsymbol{e}\} &= \int \Pr\{\boldsymbol{e}|\boldsymbol{H}\} \Pr\{\boldsymbol{H}\} \, d\boldsymbol{H} \\ &= \int Q\left(\frac{\|\boldsymbol{H}\boldsymbol{F}\boldsymbol{e}\|}{\sqrt{2}\rho}\right) \frac{1}{\pi^N \det(\boldsymbol{C})} \exp\{-\boldsymbol{h}^* \boldsymbol{C}^{-1} \boldsymbol{h}\} d\boldsymbol{h}. \end{aligned} \tag{16}$$

Using the upper bound $Q(x) \leq \frac{1}{2} \exp\left(-\frac{x^2}{2}\right)$ on the Q-function, we get

$$\begin{aligned} \Pr\{\boldsymbol{e}\} &\leq \frac{1}{2} \int \exp\left\{-\frac{\|\boldsymbol{H}\boldsymbol{F}\boldsymbol{e}\|^2}{4\rho^2}\right\} \\ &\cdot \frac{1}{\pi^N \det(\boldsymbol{C})} \exp\{-\boldsymbol{h}^* \boldsymbol{C}^{-1} \boldsymbol{h}\} d\boldsymbol{h}. \end{aligned} \tag{17}$$

Since the matrix $\boldsymbol{H}$ is diagonal, the expression $\|\boldsymbol{H}\boldsymbol{F}\boldsymbol{e}\|^2$ can be rewritten as

$$\begin{aligned} \|\boldsymbol{H}\boldsymbol{F}\boldsymbol{e}\|^2 &= (\boldsymbol{F}\boldsymbol{e})^* \text{diag}\{\boldsymbol{h}\}^* \text{diag}\{\boldsymbol{h}\}(\boldsymbol{F}\boldsymbol{e}) \\ &= \boldsymbol{h}^* \text{diag}\{\boldsymbol{F}\boldsymbol{e}\}^* \text{diag}\{\boldsymbol{F}\boldsymbol{e}\} \boldsymbol{h} \\ &= \boldsymbol{h}^* \boldsymbol{M} \boldsymbol{h}, \end{aligned} \tag{18}$$

where $\boldsymbol{f}_1, .., \boldsymbol{f}_N$ are the rows of the DFT matrix $\boldsymbol{F}$ and $\boldsymbol{M} \triangleq \text{diag}\{|\boldsymbol{f}_1 \boldsymbol{e}|^2, .., |\boldsymbol{f}_N \boldsymbol{e}|^2\}$. By substituting Eq. (18) into Eq. (17) we get

$$\begin{aligned} \Pr\{\boldsymbol{e}\} &\leq \frac{1}{2} \int \exp\left\{-\boldsymbol{h}^* \frac{\boldsymbol{M}}{4\rho^2} \boldsymbol{h}\right\} \frac{\exp\{-\boldsymbol{h}^* \boldsymbol{C}^{-1} \boldsymbol{h}\}}{\pi^N \det(\boldsymbol{C})} d\boldsymbol{h} \\ &= \frac{1}{2\pi^N \det(\boldsymbol{C})} \int \exp\left\{-\boldsymbol{h}^* \left(\frac{\boldsymbol{M}}{4\rho^2} + \boldsymbol{C}^{-1}\right) \boldsymbol{h}\right\} d\boldsymbol{h}. \end{aligned} \tag{19}$$

Since the PDF of a complex Gaussian vector $\boldsymbol{x}$ of length L with covariance $\boldsymbol{V}$ is $\frac{1}{\pi^L \det(\boldsymbol{V})} \exp\{\boldsymbol{x}^* \boldsymbol{V}^{-1} \boldsymbol{x}\}$ and its integral is 1, then Eq. (19) can be rewritten as

$$\begin{aligned} \Pr\{\boldsymbol{e}\} &\leq \frac{1}{2\det(\boldsymbol{C})} \left[\det\left(\frac{\boldsymbol{M}}{4\rho^2} + \boldsymbol{C}^{-1}\right)\right]^{-1} \\ &= \frac{1}{2} \left[\det\left(\frac{\boldsymbol{M}}{4\rho^2} \boldsymbol{C} + \boldsymbol{I}\right)\right]^{-1}. \end{aligned} \tag{20}$$

C. Uncorrelated Fading Channel

We now examine the particular case of uncorrelated Rayleigh channel. In this case, $\boldsymbol{C} = \sigma^2 \boldsymbol{I}$ and Eq. (20) becomes

$$\begin{aligned}
\Pr\{\boldsymbol{e}\} &\leq \frac{1}{2}\left[\det\left(\frac{\sigma^2}{4\rho^2}\boldsymbol{M}+\boldsymbol{I}\right)\right]^{-1} \\
&= \frac{1}{2}\left[\det\left(\frac{\sigma^2}{4\rho^2}\text{diag}\{|\boldsymbol{f}_1\boldsymbol{e}|^2,..,|\boldsymbol{f}_N\boldsymbol{e}|^2\}+\boldsymbol{I}\right)\right]^{-1} \\
&= \left(2\left(\frac{\sigma^2}{4\rho^2}|\boldsymbol{f}_1\boldsymbol{e}|^2+1\right)\cdots\left(\frac{\sigma^2}{4\rho^2}|\boldsymbol{f}_N\boldsymbol{e}|^2+1\right)\right)^{-1} \\
&= \frac{1}{2}\prod_{n=1}^{N}\left(\frac{1}{4}|\boldsymbol{f}_n\boldsymbol{e}|^2\text{SNR}+1\right)^{-1}. \qquad (21)
\end{aligned}$$

This result will be used to identify the dominant deviation vectors in both the high and the low SNR regimes.

1) *High SNR Regime*:

Let us first define the following condition:

Condition 1. A vector $\boldsymbol{e}$ is said to satisfy *Condition 1* if $\text{DFT}(\boldsymbol{e}) = \boldsymbol{F}\boldsymbol{e}$ has a single non-zero element.

Property III.1. *For any DFT of size N (a multiple of 4) there are exactly $8 \cdot 2^N$ possible QPSK transmission vectors such that for each of them there exists a deviation vector that satisfies Condition 1, with an error in a specific bit b_e.*

Justification: The rows of the DFT matrix $\left(\boldsymbol{f}_k = e^{-j\theta n}, \theta = \frac{2\pi}{N}k, n = 0,...,N-1\right)$ constitute a basis for an N-dimensional vector space. A deviation vector $\boldsymbol{e}$ can be represented by $\boldsymbol{e} = \sum_{k=0}^{N-1}(\boldsymbol{f}_k\boldsymbol{e}^*)\boldsymbol{f}_k$. Therefore, for $\boldsymbol{e}$ to satisfy Condition 1, it necessarily means that it must be "spanned" by a single basis vector. It follows that $\boldsymbol{e}$ can only be one of the DFT matrix rows (up to a constant multiplication). Only four rows of F are relevant in this context. These are

$$\begin{aligned}
&1 \quad 1 \quad 1 \quad 1 \quad ... \quad 1 \quad 1, \\
&1 \quad j \quad -1 \quad -j \quad ... \quad -1 \quad -j, \\
&1 \quad -1 \quad 1 \quad -1 \quad ... \quad 1 \quad -1, \\
&1 \quad -j \quad -1 \quad j \quad ... \quad -1 \quad j.
\end{aligned} \qquad (22)$$

which correspond to $\theta = 0$, $\theta = \frac{\pi}{2}$, $\theta = \pi$ and $\theta = \frac{3\pi}{2}$, respectively.

Let Λ be the set of length-N vectors of QPSK symbols. In addition, assume that $\boldsymbol{c} \in \Lambda$. There can be $2 \cdot 2^N$ source vectors $\boldsymbol{c}$ (out of the 4^N possible vectors in Λ) such that $\boldsymbol{c} + \mu \cdot \boldsymbol{e} \in \Lambda$, where $\boldsymbol{e}$ is one of the above 4 deviation vectors (the rows of the DFT matrix given in Eq. (22)) and $\mu \in \{\pm 1, \pm j, \pm 1 \pm j\}$. The value $2 \cdot 2^N$ can be explained as follows: 2 stands for two values of b_e, and 2^N stands for the second bit from the QPSK symbols. Hence, the total are $4 \cdot 2 \cdot 2^N = 8 \cdot 2^N$ possible QPSK transmission vectors such that for each of them there exists a deviation vector satisfying Condition 1 with an error in the specific bit b_e.

Theorem III.2. *In the high SNR regime, a lower bound for the ML detection of SC-FDMA for an uncoded QPSK is given by*

$$\lim_{SNR\to\infty} P_b^{(QPSK,MLD)} = \frac{4}{N2^N\, SNR}, \tag{23}$$

and the diversity order is 1.

Proof: For high SNR, the deviation vector with the smallest diversity order (DO) dominates the error probability [12]. The DO is defined in [12] to be

$$\text{DO} \triangleq -\lim_{\text{SNR}\to\infty} \frac{\log_e \Pr\{\text{error}\}}{\log_e \text{SNR}}. \tag{24}$$

The DO, which is associated with $\Pr\{\boldsymbol{e}\}$, is computed by using Eqs. (24) and (21)

$$\begin{aligned} \text{DO}\{\Pr\{\boldsymbol{e}\}\} &= -\lim_{\text{SNR}\to\infty} \frac{1}{\log_e \text{SNR}} \log_e \Pr\{\boldsymbol{e}\} \\ &\geq \lim_{\text{SNR}\to\infty} \frac{1}{\log_e \text{SNR}} \log_e 2 \prod_{n=1}^{N} \left(\frac{1}{4}|\boldsymbol{f}_n\boldsymbol{e}|^2\text{SNR}+1\right) \\ &\geq \lim_{\text{SNR}\to\infty} \frac{1}{\log_e \text{SNR}} \log_e 2 \prod_{n:\boldsymbol{f}_n\boldsymbol{e}\neq 0} \frac{1}{4}|\boldsymbol{f}_n\boldsymbol{e}|^2 \\ &+ \lim_{\text{SNR}\to\infty} \frac{\log_e \text{SNR}^K}{\log_e \text{SNR}} = K, \end{aligned} \tag{25}$$

where K is the number of non-zero elements in $\boldsymbol{F}\boldsymbol{e}$. From Eq. (25) we conclude that the DO, which is associated with $\Pr\{\boldsymbol{e}\}$, is greater or equal to the number of non-zero elements in $\boldsymbol{F}\boldsymbol{e}$.

Specifically, the deviation vector $\boldsymbol{e}_x$, which satisfies Condition 1, has the following probability

$$\begin{aligned} \Pr\{\boldsymbol{e}_x\} &= \int \Pr\{\boldsymbol{e}_x|\boldsymbol{H}\} \Pr\{\boldsymbol{H}\}\, d\boldsymbol{H} \\ &= \int Q\left(\frac{\|\boldsymbol{H}\boldsymbol{F}\boldsymbol{e}_x\|}{\sqrt{2}\rho}\right) P(\boldsymbol{H}) d\boldsymbol{H} \\ &= \int Q\left(\sqrt{N\,\text{SNR}}\cdot y\right) 2y\exp(-y^2) dy, \end{aligned} \tag{26}$$

where $y = |h|$ is a normalized Rayleigh distributed scalar and $\text{SNR} = 1/\rho^2$. Equation (26) is a standard Q-function integral w.r.t. Rayleigh distribution function [13]

$$\int_0^\infty Q(ay) P_{Rayleigh}(y)\, dy = \frac{1}{2}\left(1 - \frac{1}{\sqrt{1+\frac{2}{a^2}}}\right) \geq \frac{1}{2a^2}.$$

Substituting the argument $a = \sqrt{N\,\text{SNR}}$ yields a tight bound for moderate and high SNR values:

$$\Pr\{\boldsymbol{e}_x\} \geq \frac{1}{2N\,\text{SNR}}. \tag{27}$$

The DO associated with Eq. (27) is

$$\mathrm{DO}\{\Pr\{\boldsymbol{e}_x\}\} \quad = \quad \lim_{\mathrm{SNR}\to\infty} \frac{\log_e 2N\,\mathrm{SNR}}{\log_e \mathrm{SNR}} = 1. \tag{28}$$

From Eqs. (28) and (25) it follows that $\boldsymbol{e}_x$, which satisfies Condition 1, produces the error probability associated with the smallest DO. Therefore, it dominates the error probability in the high SNR regime. This can be verified by comparing the two probabilities P_1 and P_2 associated with the diversity orders $\mathrm{DO}_1 < \mathrm{DO}_2$ when the SNR tends to infinity:

$$\lim_{\mathrm{SNR}\to\infty} (\log \mathrm{P}_1 - \log \mathrm{P}_2) = -\lim_{\mathrm{SNR}\to\infty} (\mathrm{DO}_1 - \mathrm{DO}_2) \log \mathrm{SNR} = \infty\,.$$

In order to obtain an explicit lower bound on the bit error probability, we must take into account that not all the possible deviation vectors are valid for a given transmitted vector $\boldsymbol{s}$. For example, all the elements in the deviation vector $\boldsymbol{e}$ may be equal to 2 with non-zero probability, only if all the elements of the transmitted vector $\boldsymbol{s}$ are equal to -1. Property (III.1) states that for QPSK there are exactly $8 \cdot 2^N$ possible deviation vectors of length N that satisfy Condition 1. In other words, the probability of transmitting a vector with DO=1 is $\frac{8 \cdot 2^N}{4^N} = \frac{8}{2^N}$. Using Eq. (15), we multiply Eq. (27) by this factor and we get that the MLD bit-error probability for SC-FDMA in an uncorrelated Rayleigh fading channel is lower bounded by

$$\mathrm{P}_b^{(\mathrm{QPSK,MLD})}(\text{high SNR}) \geq \frac{8}{2^N} \frac{1}{2N\,\mathrm{SNR}} = \frac{4}{N 2^N\,\mathrm{SNR}}.$$

■

We can see from Eq. (23) that the diversity gain increases (and the error probability curve shifts to the left) as N, the DFT size, increases. This is true in the setting used in this work, i.e. an uncoded transmission over an uncorrelated fading channel. In a practical system such as OFDMA, the channel diversity will be utilized by means of interleaving, coding and allocation techniques. Therefore, the performance difference between OFDMA and SC-FDMA with different DFT sizes is expected to be small.

In the simpler case of BPSK, the number of rows in Equation (22) is reduced to two (only real values) and the expression in Eq. (23) is divided by 2 (the two QPSK bits are orthogonal), yielding

$$\mathrm{P}_b^{(\mathrm{BPSK,MLD})}(\text{high SNR}) \geq \frac{4}{2^N} \frac{1}{4N\,\mathrm{SNR}} = \frac{1}{N 2^N\,\mathrm{SNR}}.$$

*2) **Low SNR Regime**:*

Returning to Eq. (16), we employ the following lower bound for the Q-function [14]

$$Q(x) = \frac{1}{2}\text{erfc}\left(\frac{x}{\sqrt{2}}\right) > \frac{1}{2}0.56\exp\left\{-1.275\frac{x^2}{2}\right\}.$$

Substituting it into Eq. (16), then following the line of proof leading from Eq. (16) to Eq. (20), we obtain the lower bound for $\Pr\{\boldsymbol{e}\}$ to be:

$$\Pr\{\boldsymbol{e}\} \quad > \quad 0.28\left[\det\left(1.275\frac{\text{diag}\{|\boldsymbol{f}_1\boldsymbol{e}|^2,..,|\boldsymbol{f}_N\boldsymbol{e}|^2\}}{4\rho^2}\boldsymbol{C}+\boldsymbol{I}\right)\right]^{-1}. \tag{29}$$

In order to identify the dominant deviation vector at the low SNR regime, we rewrite Eq. (21) as follows

$$\begin{aligned}\Pr\{\boldsymbol{e}\} &\leq \frac{1}{2}\prod_{n=1}^{N}\left(\frac{1}{4}|\boldsymbol{f}_n\boldsymbol{e}|^2\text{SNR}+1\right)^{-1} = \frac{1}{2}\frac{1}{\left(\frac{1}{4}|\boldsymbol{f}_1\boldsymbol{e}|^2\text{SNR}+1\right)\cdot...\cdot\left(\frac{1}{4}|\boldsymbol{f}_N\boldsymbol{e}|^2\text{SNR}+1\right)} \\ &= \frac{1}{2}\frac{1}{1+\sum_{n=1}^{N}\frac{1}{4}|\boldsymbol{f}_n\boldsymbol{e}|^2\text{SNR}+\sum_{n=1}^{N}\sum_{k=1:k\neq n}^{N}(\frac{1}{4})^2|\boldsymbol{f}_n\boldsymbol{e}|^2|\boldsymbol{f}_k\boldsymbol{e}|^2\text{SNR}^2+...+\prod_{n=1}^{N}\frac{1}{4}|\boldsymbol{f}_n\boldsymbol{e}|^2\text{SNR}} \\ &\leq \frac{1}{2\left(1+\sum_{n=1}^{N}\frac{1}{4}|\boldsymbol{f}_n\boldsymbol{e}|^2\text{SNR}\right)} = \frac{1}{2\left(1+\frac{1}{4}\text{SNR}\|\boldsymbol{e}\|^2\right)},\end{aligned} \tag{30}$$

where the last inequality is attributed to the fact that SNR^n is negligible in comparison to SNR, when SNR is sufficiently small and $n \geq 2$.

Clearly, the bound in Eq.(30) obtains its maximum value when the deviation vector e is of minimum norm. Consequently, the dominant deviation vectors in the low SNR regime are those that have a single non-zero element. Hence, by substituting, e.g. $\boldsymbol{e} = [\sqrt{2}, 0, ..., 0]$ and $\boldsymbol{f}_1, .., \boldsymbol{f}_N$ into (29), we get that the lower bound for the BER in the low SNR regime is

$$\text{P}_b^{(\text{QPSK,MLD})}(\text{low SNR}) > 0.28\left(1+0.6375\frac{\text{SNR}}{N}\right)^{-N}. \tag{31}$$

Note that this lower bound has a performance slope respective to the diversity order N.

In the BPSK case, the distance between the constellation points is smaller by a factor of $\sqrt{2}$. Therefore, the lower bound becomes

$$\text{P}_b^{(\text{BPSK,MLD})}(\text{low SNR}) > 0.28\left(1+1.275\frac{\text{SNR}}{N}\right)^{-N}. \tag{32}$$

The bounds (31) and (32) are validated by the simulation.

D. Correlated Fading Channel

In a correlated Rayleigh channel with correlation matrix $\boldsymbol{C}$, the deviation vector associated with the smallest DO is the same as in the uncorrelated case Eq. (23). This is because the substitution of a deviation vector, which satisfies Condition 1, into Eq. (20) yields a linear expression in the SNR, hence, DO=1. For example, by substituting $\boldsymbol{e} = [\sqrt{2}, \sqrt{2}, ..., \sqrt{2}]$ into the determinant in Eq. (20), we get

$$\begin{aligned} & \det\left(\frac{\text{diag}\{|\boldsymbol{f}_1\boldsymbol{e}|^2, \ldots, |\boldsymbol{f}_N\boldsymbol{e}|^2\}}{4\rho^2}\boldsymbol{C} + \boldsymbol{I}\right) = \\ = \quad & \det\begin{bmatrix} \frac{N}{2}\cdot\text{SNR}+1 & \frac{N}{2}c_{1,2}\text{SNR} & ... & \frac{N}{2}c_{1,N}\text{SNR} \\ 0 & 1 & ... & 0 \\ ... & ... & ... & ... \\ 0 & 0 & ... & 1 \end{bmatrix} \\ = \quad & \frac{N}{2}\cdot\text{SNR}+1. \end{aligned} \tag{33}$$

For any (other) non-zero deviation vector that does not satisfy Condition 1, Eq. (33) becomes a polynomial equation of degree at least 2 of the SNR. Consequently, the corresponding BER will be affected by DO of at least 2. Therefore, when $\det(\boldsymbol{C}) \neq 0$, the asymptotical lower bound of the BER for a correlated Rayleigh channel is the same as that of the uncorrelated Rayleigh channel in Eq. (23).

Let us examine a flat fading Rayleigh channel, which is a particular channel example where $\det(\boldsymbol{C}) = 0$. In this case, Eq. (16) no longer holds since the distribution function contains division by $\det(\boldsymbol{C})$. Instead, we can rewrite Eq. (10) for a flat fading case $\boldsymbol{H} = h \cdot \boldsymbol{I}$, where h is a complex scalar with a Gaussian distribution. Hence,

$$\begin{aligned} \Pr\{\boldsymbol{e}|\boldsymbol{H}\} &= Q\left(\frac{\|\boldsymbol{H}\boldsymbol{F}\boldsymbol{e}\|}{\sqrt{2}\rho}\right) = Q\left(\frac{|h|\cdot\|\boldsymbol{F}\boldsymbol{e}\|}{\sqrt{2}\rho}\right) \\ &= Q\left(\frac{|h|\cdot\|\boldsymbol{e}\|}{\sqrt{2}\rho}\right). \end{aligned} \tag{34}$$

Therefore,

$$\text{P}_b \approx \Pr\{\boldsymbol{e} : \text{single non zero element}|\boldsymbol{H}\} = Q\left(\sqrt{\text{SNR}}\right), \tag{35}$$

which is similar to the BER expression in OFDM (Eq. (12)). Since the performance of SC-FDMA in a Rayleigh channel can only be better than those obtained in a flat fading channel, one can use the OFDM BER performance for upper bounding the BER performance of SC-FDMA.

It follows from the above derivation, which is validated in Fig. 1, that the BER curves for ML detected SC-FDMA over a Rayleigh channel are upper bounded by the OFDM BER performance in Eq. (35) and lower bounded by Eq. (23).

IV. Simulation Results

In order to validate the performance predicted by Eqs. (23) and (31), we conducted a Monte-Carlo simulation study. We used the ML detection for SC-FDMA with DFT of sizes of 2,4,8 in an uncorrelated Rayleigh fading channel. $3.2 \cdot 10^6$ bits were transmitted for each SNR point. In addition, the matched filter bound (see [1] and [15]), which is denoted in the figures by MFB, was used as a reference. The empirical performance of the MLD and the analytical bounds together with the referenced MFB are shown in Fig. 1.

Evidently, the empirical BER curves converge for the lower bound in the high SNR regime. Note that although the MFB is close to the lower bound in the low SNR regime, it does not predict the low diversity order of the MLD in the high SNR regime. This is due to the fact the MFB ignores inter-symbol interference.

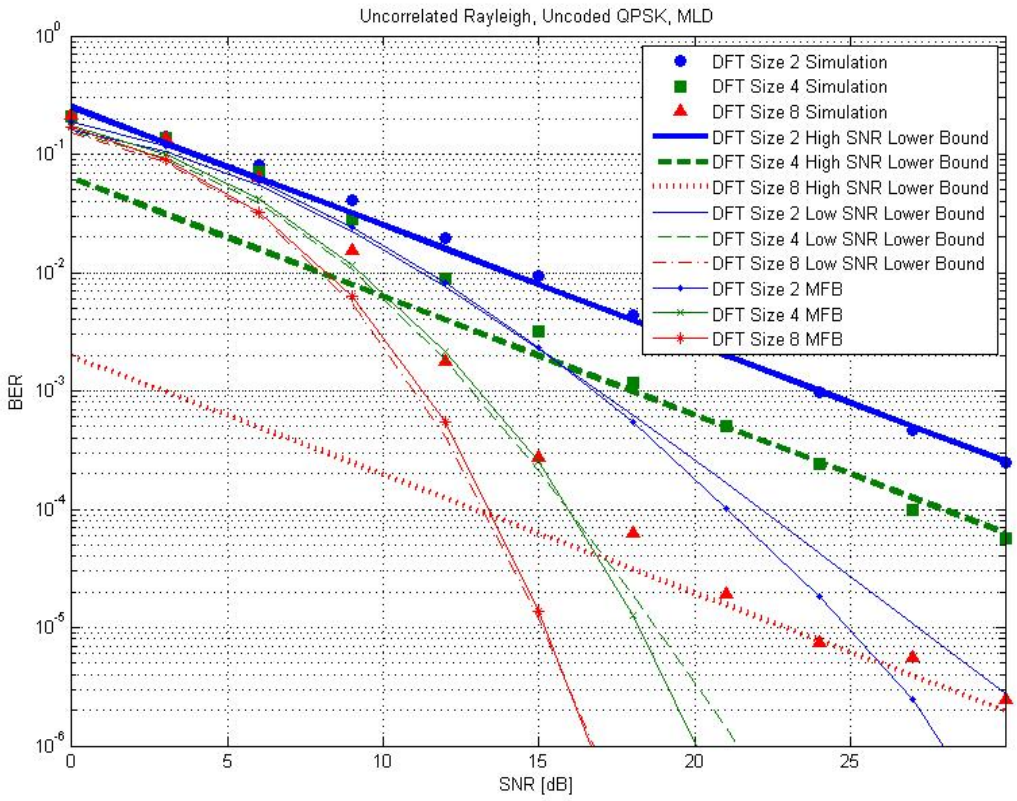

Fig. 1. BER of ML detected SC-FDMA (DFT of sizes 2,4,8) over an uncorrelated Rayleigh channel using an uncoded QPSK modulation.

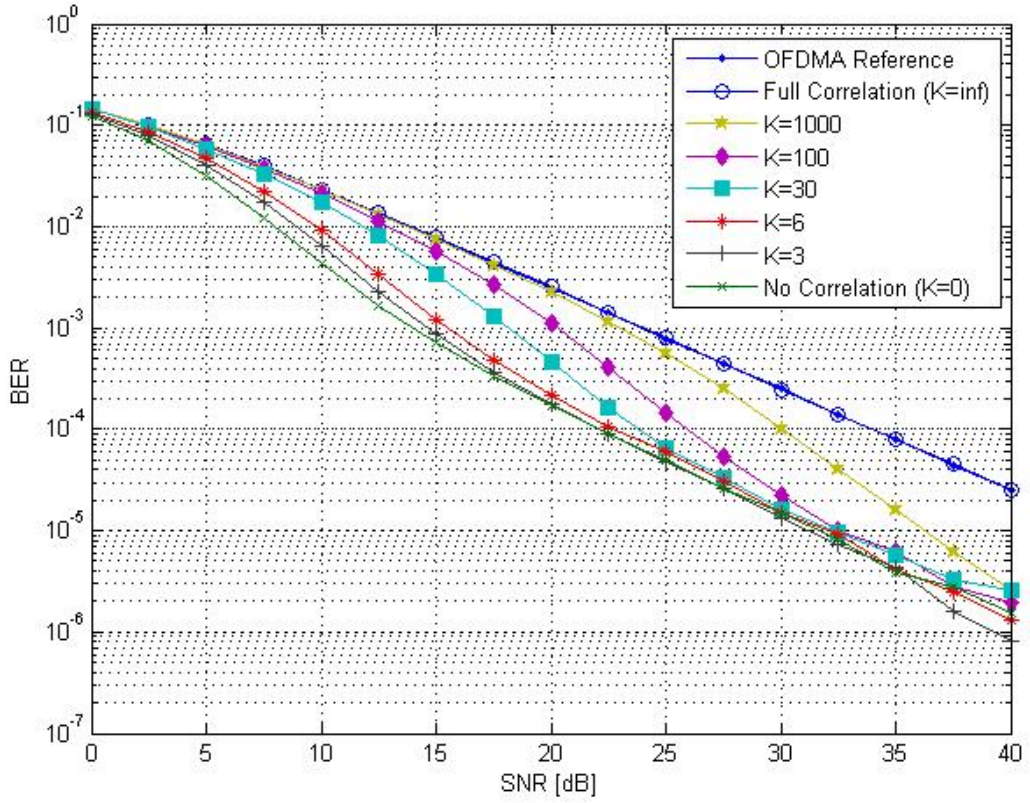

Fig. 2. BER of MLD applied to SC-FDMA (DFT of size 4) over a correlated Rayleigh channel using an uncoded BPSK modulation. The correlation function is $r[n] = \exp\{-\frac{n}{K}\}$, where n is the sub-carrier index and K is a constant.

The effect of frequency domain correlation on the BER is demonstrated in Fig. 2. The top curve, which is used here as a reference, presents the BER performance of the OFDM. All the other curves correspond to the BER performance of ML-detected SC-FDMA (DFT of size 4) in a Rayleigh fading channel with the correlation function $r[n] = \exp\{-n/K\}$, where n is the difference between the sub-carrier indices and K is the fading-channel correlation parameter. We studied the correlation function for the following values of the parameter $K = 3$, 6, 30, 100, 1000. From Fig. 2, we conclude that the BER curve for the Rayleigh fading channel, with the correlation function defined above, is upper bounded by the OFDM BER curve (Eq. (35)) and lower bounded by the lower bound in the high SNR regime (Eq. (23)). Moreover, all the curves except the one that corresponds to fully correlated fading channel, converge to the lower bound in the high SNR regime.

Employing MLD for QPSK with large DFT sizes is impractical due to its high computational complexity. Thus, when addressing larger DFT sizes, we used the BPSK modulation and employ the near-optimum QRM-MLD algorithm

with a sufficiently large parameter M [16]. The performance of QRM-MLD for DFT of sizes 12 and 32 with $3.2 \cdot 10^6$ bits per SNR point is demonstrated in Figs. 3 and 4, respectively.

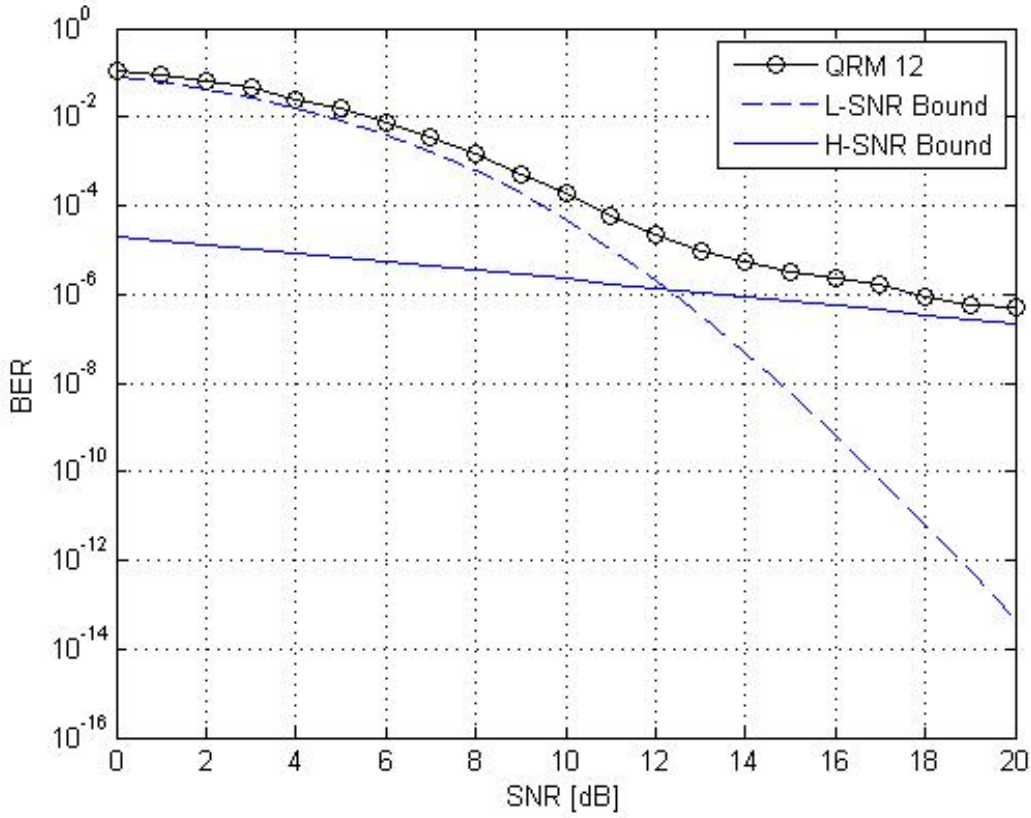

Fig. 3. BER of QRM-MLD (with $M = 12$) applied to SC-FDMA with 16 point DFT and BPSK in an uncorrelated Rayleigh channel.

The simulation results reveal that the derived bounds are in a good agreement with the performance of QRM-MLD when a sufficiently large parameter M is used for both low and high SNR values. This in turn means that the performance of the QRM-MLD reduced-complexity is close to the optimal ML. Moreover, the intersection point between the bounds predicts the SNR region where the slope of the BER curve drops from N to 1.

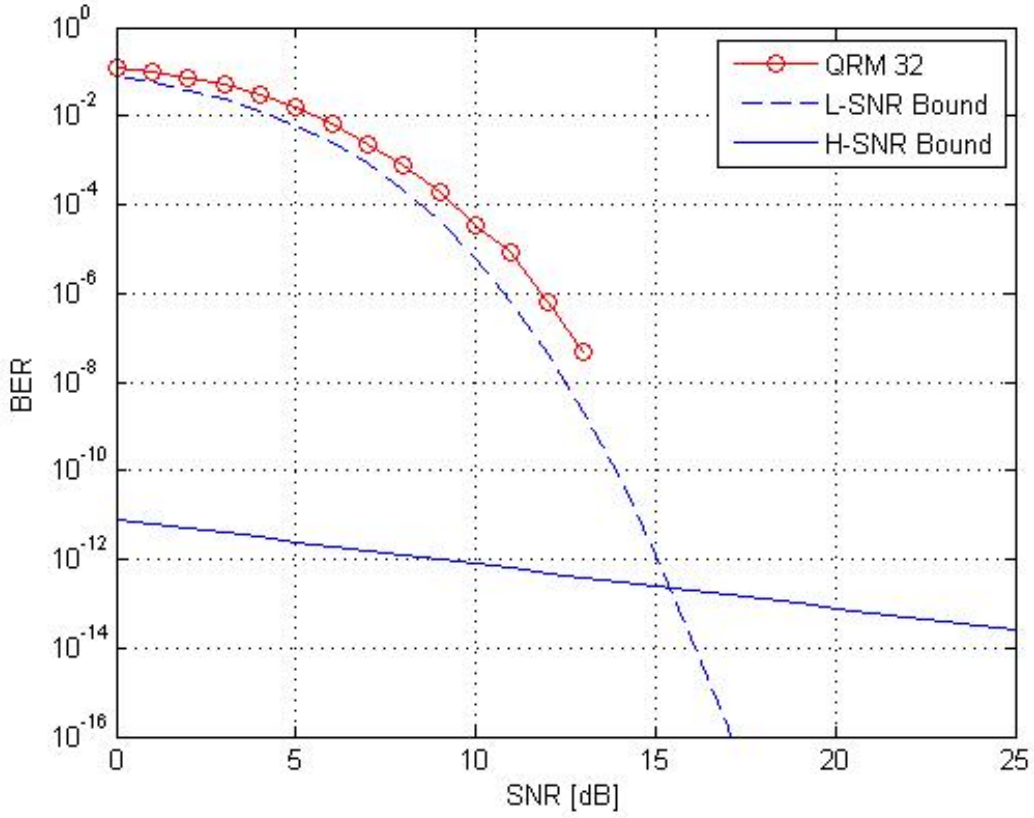

Fig. 4. BER of QRM-MLD (with $M = 32$) applied to SC-FDMA with 32 point DFT and BPSK in an uncorrelated Rayleigh channel.

V. Discussion and Conclusions

In this paper, the derivation of lower bounds on the bit error probability for ML detection of SC-FDMA transmission in uncorrelated and correlated Rayleigh fading channel is presented. The results may serve as performance bounds for advanced SC-FDMA detection schemes. In the case of an uncorrelated Rayleigh fading channel, the bounds show that the slope of the BER curve for the low SNR regime is significantly higher than in high SNR revealing BER flaring behavior.

It is also demonstrated that the BER value in which the slope changes corresponds to the DFT size. Specifically, the larger the DFT size is, the smaller is the BER value at which the slope changes. The flaring behavior appears when the DFT size is small and the correlation in the frequency domain is small (e.g., in distributed SC-FDMA). In coded systems, the error floor behavior is expected in the conditions above at high coding rates where the working SNR is high.

Acknowledgement. The authors thank the anonymous reviewers for their constructive comments and suggestions.

REFERENCES

[1] N.Benvenuto, R.Dinis, D.Falconer and S.Tomasin, "Single Carrier Modulation with Non Linear Frequency Domain Equalization: An Idea Whose Time Has Come - Again," *IEEE Proceedings*, Jan 2010.

[2] R. Koetter, A.C. Singer and M. Tuchler, "Turbo equalization," *IEEE Signal Processing Mag.*, vol. 21, no. 1, pp. 67–80, 2004.

[3] M. Tuchler and J. Hagenauer, "Turbo equalization using frequency domain equalizers," *Proc. Allerton Conference, Monticello, AR, USA*, vol. 8, no. 6, pp. 144–153, 2000.

[4] G. Berardinelli, B.E. Priyanto, T.B. Sorensen and P. Mogensen, "Improving SC-FDMA Performance by Turbo Equalization in UTRA LTE Uplink," *IEEE Vehicular Technology Conference 2008*, pp. 2557 – 2561, 2008.

[5] L. Charrua, P. Torres, V. Goncalves and A. Gusmao, "Iterative receiver techniques for SC-FDMA uplink block transmission: design and performance evaluation," *IEEE conference on Global telecommunications 2009*, pp. 1648–1654, 2009.

[6] N. Prasad, S. Wang and X. Wang, "Efficient Receiver Algorithms for DFT-Spread OFDM Systems," *IEEE Trans. Wireless Comm.*, vol. 8, no. 6, pp. 3216–3225, 2009.

[7] H. Wang, X. You, B. Jiang and X. Gao, "Performance Analysis of Frequency Domain Equalization in SC-FDMA Systems," *IEEE International Communications Conference*, pp. 4342–4347, 2008.

[8] M.D. Nisar, H. Nottensteiner, T. Hindelang, "On Performance Limits of DFT Spread OFDM Systems," *Mobile and Wireless Communications Summit*, pp. 1–4, 2007.

[9] M. Geles, A. Averbuch, O. Amrani, and D. Ezri, "Maximum Likelihood Detection for Single Carrier - FDMA: Performance Analysis," *IEEE 26-th Convention of Electrical and Electronics Engineers in Israel*, 2010.

[10] D. Tse and P. Viswanath, *Fundamental of Wireless Communication*. Cambridge University Press, 2005.

[11] S. Haykin and M. Moher, *Modern Wireless Communication*. Prentice-Hall, Inc., 2004.

[12] A. Paulraj, R. Nabar and D. Gore, *Introduction to Space Time Wireless Communications*. Cambridge University Press, 2003.

[13] A. Goldsmidt, *Wireless Communication*. Cambridge University Press, 2005.

[14] N.Ermolova and S.-G.Haggman, "Simplified Bounds for the Complementary Error Function; Applicaiton to the Performance Evaluation of Signal Processing Systems," *12-th European Signal Processing Conference*, pp. 1087– 1090.

[15] N.Benvenuto and S.Tomasin, "Iterative Design and Detection of a DFE in the Frequency Domain," *IEEE Transactions on Communication*, vol. 53, no. 11, Nov 2005.

[16] T. Miyatani, "Frequency-Domain QR-Decomposed and Equalized MLD for Single-Carrier MIMO Systems over Multipath Fading Channels," *IEICE Transactions on Communications*, vol. E91B, no. 6, pp. 2052–2058, 2008.